

## Simulation of Self-propulsive Phenomenon, Using Lattice Boltzmann Method

M. Beigzadeh-Abbassi<sup>1</sup>, M.R. Beigzadeh-Abbassi<sup>2</sup>

<sup>1</sup>Mechanical Engineering Department, Sirjan University of Technology, Sirjan, Iran

<sup>2</sup>Aerospace Engineering Department, Sharif University of Technology, Tehran, Iran  
[m.r.beigzadeh@gmail.com](mailto:m.r.beigzadeh@gmail.com)

**Abstract:** Many human inventions are inspired by nature, such as fish swimming, bird/insect flight, etc. A basic consideration for the design of swimming machines is the design of propulsors. A creative design of propulsors can be inspired by fish locomotion. The term locomotion means that thrust is generated by undulation of fish body. Thus, there is no need to have an external propulsor. In this study, sub-carangiform motion, which is a well known locomotion and which is practiced by most fish, is simulated numerically using Lattice Boltzmann method (LBM). To simulate the geometry of fishlike body, the profile of a flexible NACA 0012 airfoil was used. Note, we deal here with an incompressible unsteady flow. Also, the results show that lattice Boltzmann method, accompany with modified boundary conditions for curved solid boundaries, can accurately simulate the variation of drag coefficient with time. The velocity profiles and vortex structures are shown to be close to other reliable numerical results. The results show vortex pairs in the wake of the oscillating flexible airfoil, which are very similar to Von-Kármán vortices. Also, the results show that lattice Boltzmann method, accompany with modified boundary conditions for curved solid boundaries, can accurately simulate the variation of drag coefficient with time.

[M. Beigzadeh-Abbassi, M.R. Beigzadeh-Abbassi. **Simulation of Self-propulsive Phenomenon, Using Lattice Boltzmann Method.** Journal of American Science 2012; 8(2):304-309]. (ISSN: 1545-1003). <http://www.americanscience.org>. 43

**Keywords:** Lattice Boltzmann method; Curved Boundary Condition; Bounce-back Boundary Condition; Unsteady Flow

### 1. Introduction

Understanding self-propulsive phenomena which are practiced by fish can give us innovations for designing under water vehicles. Locomotion of fish has been always a matter of respect because of its diverse, complicated and interesting nature. Types of locomotion of fish vary according to the body structures, fin structures and the locations of fins on fish bodies.

In this paper we are going to model the locomotion of a fish-like body via simulating an unsteady incompressible fluid flow using lattice Boltzmann method. This paper has two objectives:

(a) Physical Aspect: the main objective of this paper is to simulate a self-propulsive phenomenon which is practiced by some kind of fish known as carangiform motion, and

(b) Numerical aspect: The present study needs a numerical tool which holds some important features, such as: (1) A high order of accuracy at the same time a simple implementation, (2) An appropriate computational speed, and (3) The ability to simulate fluid flows over arbitrary bodies.

Lattice Boltzmann method has all these features but it also suffers from deficiencies which needs to be optimized. As far as we know, a study in which locomotion is simulated using lattice Boltzmann method has not been published yet.

### 2. Lattice Boltzmann Method

Lattice boltzmann method has been constructed according to dynamics of particles and uses Boltzmann equation which has a mesoscopic concept (a concept between microscopic and macroscopic) instead of using Navier-stokes equations which has a macroscopic basis [5]. Spacial and temporal differencing of Boltzmann equation and resulting to lattice Boltzmann equation has been summarized in the following. Beginning from Boltzmann equation we have [6]:

$$\frac{Df_{\alpha}}{Dt} = \frac{\partial f_{\alpha}}{\partial t} + \mathbf{e}_{\alpha} \cdot \nabla f_{\alpha} = \Gamma^{(+)} - \Gamma^{(-)}. \quad (1)$$

Using Bhatnagar-Gross-Krook (BGK) approximation, the collision operator has been linearized:

$$\frac{Df_{\alpha}}{Dt} = \frac{\partial f_{\alpha}}{\partial t} + \mathbf{e}_{\alpha} \cdot \nabla f_{\alpha} = -\frac{1}{\lambda} (f_{\alpha} - f_{\alpha}^{(eq)}), \quad (2)$$

where  $f_{\alpha}^{(eq)}$  is Maxwell-boltzmann equilibrium function. Using finite difference, the material derivative in the left hand side of equation (2) is differenced as:

$$\frac{Df_{\alpha}}{Dt} = \frac{f_{\alpha}(\mathbf{x} + \mathbf{e}_{\alpha} \Delta t, t + \Delta t) - f_{\alpha}(\mathbf{x}, t)}{\Delta t} = -\frac{1}{\lambda} (f_{\alpha} - f_{\alpha}^{(eq)}). \quad (3)$$

By introducing non-dimensional relaxation time, lattice Boltzmann equation is derived [6]:

$$\tau = \Delta t / \lambda, \quad (4)$$

$$f_\alpha(\mathbf{x} + \mathbf{e}_\alpha \Delta t, t + \Delta t) - f_\alpha(\mathbf{x}, t) = -\frac{1}{\tau} (f_\alpha - f_\alpha^{(eq)}). \quad (5)$$

Equation (5) is known as lattice Boltzmann equation, which is separated into two steps to be solved numerically. One step is the collision step (right hand side of equation (5)) and the other is the streaming step (left hand side of equation (5)) of the distribution function ( $f$ ). Density and velocity of the fluid can be obtained from distribution functions by these equations [7]:

$$\rho = \sum_{\alpha=0}^8 f_\alpha, \quad (6)$$

$$\mathbf{u} = \frac{1}{\rho} \sum_{\alpha=0}^8 f_\alpha \mathbf{e}_\alpha. \quad (7)$$

### 2.1. Two-Dimensional Model Using D2Q9 Lattice

D2Q9 lattice uses a two-dimensional nine-velocity lattice. This method has been introduced by Qian et al. (1992). In this model particles are allowed to reside only on lattice nodes. The velocities of particles are limited to three values and their directions are limited to eight values [8] (figure 1).

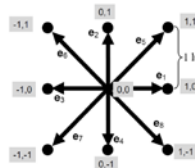


Figure 1. D2Q9 x, y velocity components [6]

### 2.2. FH Boundary Condition

The fraction of the intersected link in the fluid region is [4]:

$$\Delta = \frac{|\mathbf{x}_f - \mathbf{x}_w|}{|\mathbf{x}_f - \mathbf{x}_b|}, \quad (8)$$

which is illustrated in Figure 2.

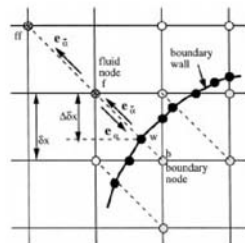


Figure 2. Cartesian two-dimensional lattices and solid curved boundary [2]

To finish the streaming step, it is clear that  $\tilde{f}_\alpha(\mathbf{x}_b, t)$  should be calculated and then substituted as:

$$f_\alpha(\mathbf{x}_f = \mathbf{x}_b + \mathbf{e}_\alpha \delta t, t + \delta t) = \tilde{f}_\alpha(\mathbf{x}_b, t). \quad (9)$$

Filippova and Hanel have obtained the value of  $\tilde{f}_\alpha(\mathbf{x}_b, t)$  by using a linear interpolation of the information of neighboring nodes:

$$\tilde{f}_\alpha(\mathbf{x}_b, t) = (1 - \chi) \tilde{f}_\alpha(\mathbf{x}_f, t) + \chi f_\alpha^{(*)}(\mathbf{x}_b, t), \quad (10)$$

where  $f_\alpha^{(*)}(\mathbf{x}_b, t)$  is known as fictitious equilibrium function and is defined by the following equation:

$$f_\alpha^{(*)}(\mathbf{x}_b, t) = \omega_\alpha \rho(\mathbf{x}_f, t) \left[ 1 + \frac{3}{c^2} \mathbf{e}_\alpha \cdot \mathbf{u}_{bf} + \frac{9}{2c^4} (\mathbf{e}_\alpha \cdot \mathbf{u}_f)^2 - \frac{3}{2c^2} \mathbf{u}_f \cdot \mathbf{u}_f \right], \quad (11)$$

where the parameter  $\omega_i$  is a weighting factor specific for each velocity direction. In the case of the D2Q9,  $\omega_0 = 4/9$ ,  $\omega_1 = 1/9$ , and  $\omega_2 = 1/36$  where  $\omega_0$  is the coefficient for the rest velocity,  $\omega_1$  is the coefficient for velocity directions with a magnitude of one (1, 2, 3, and 4 in this case), and  $\omega_2$  is the coefficient for velocity directions with a magnitude of  $\sqrt{2}$  (5, 6, 7, and 8 in this case). The value of  $c$  is defined as,  $c = \Delta x / \Delta t$ , which has a magnitude of one in this model.

Filippova and Hanel have introduced the values of  $\chi$  and  $\mathbf{u}_{bf}$  for different values of  $\Delta$ :

$$\mathbf{u}_{bf} = (\Delta - 1) \mathbf{u}_f / \Delta + \mathbf{u}_w / \Delta, \quad \chi = (2\Delta - 1) / \tau, \quad (12)$$

$$\text{for } \Delta \geq 1/2, \quad (13)$$

and

$$\mathbf{u}_{bf} = \mathbf{u}_f, \quad \chi = (2\Delta - 1) / (\tau - 1), \quad (14)$$

$$\text{for } \Delta \leq 1/2. \quad (15)$$

### 2.3. Zou, Q and He, X. Boundary Condition on a Flow Boundary with Fixed Velocity

Suppose a flow boundary (take the inlet in Figure 3 as example) is along the  $y$ -direction, and the pressure (density) is to be specified on it. After streaming,  $f_2, f_3, f_4, f_6$  and  $f_7$  are known,  $u_x$  and  $u_y$  are specified at inlet. (the velocity profile is the velocity profile of a poisson flow).

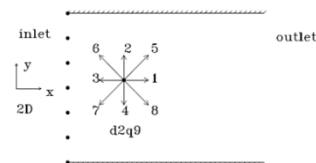


Figure 3. Boundary nodes in inlet boundary for a two-dimensional channel flow [10]

By solving the four equations obtained from equations of mass, momentum and the equation obtained from bounce-back rule for the non-equilibrium part of the particle distribution normal to

the inlet, density and other unknown distribution functions are obtained:

$$\rho = \frac{1}{1-u_x} [f_0 + f_2 + f_4 + 2(f_3 + f_6 + f_7)], \quad (16)$$

$$f_1 = f_3 + \frac{2}{3} \rho u_x, \quad (17)$$

$$f_5 = f_7 - \frac{1}{2}(f_2 - f_4) + \frac{1}{2} \rho u_y + \frac{1}{6} \rho u_x, \quad (18)$$

$$f_8 = f_6 + \frac{1}{2}(f_2 - f_4) - \frac{1}{2} \rho u_y + \frac{1}{6} \rho u_x. \quad (19)$$

**2.4. Calculating the Force on a Body**

By using the momentum-exchange method presented by Ladd & Verberg the force exerted on a surface by fluid can be evaluated [11]. The force exerted on a boundary can be evaluated using the distribution function after the collision step and the momentum exchange term which relates to the object velocity (figure 4).

$$\mathbf{F}(\mathbf{x}_w, t + \frac{1}{2} \Delta t) = \frac{\Delta x^3}{\Delta t} [2f_i^c(\mathbf{x}_A, t) - \frac{2w_i \rho(\mathbf{u}_w \cdot \mathbf{e}_i)}{c_s^2}] \mathbf{e}_i. \quad (20)$$

where the parameter  $w_i$  is a weighting factor.

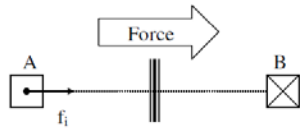


Figure 4. Illustration of the Momentum-Exchange Method for Force Evaluation (fluid exists only outside of wall) [11]

In order to get the total force and torque on a solid moving particle immersed in fluid, a summation of the forces is done around the boundary of a particle [11]:

$$\mathbf{F}_{total}(t + \frac{1}{2} \Delta t) = \sum \mathbf{F}(\mathbf{x}_w, t + \frac{1}{2} \Delta t), \quad (21)$$

$$\mathbf{T}_{total}(t + \frac{1}{2} \Delta t) = \sum (\mathbf{x}_w - \mathbf{x}_{CM}) \times \mathbf{F}(\mathbf{x}_w, t + \frac{1}{2} \Delta t). \quad (22)$$

In order to compare different boundary conditions with each other for a moving solid curved boundary at first we compare these boundary conditions for a stationary solid curved boundary.

**3. Unsteady Flow due to Translational and Rotational Oscillation of a Circular Cylinder**

In this part, unsteady flow over a translational and rotational oscillating circular cylinder with a phase difference between translational and rotational movements is going to be modeled. The mechanism of the flow due to this motion is the same as the mechanism due to locomotion of swimming

objects. If both motions are simple harmonic, the flows are characterized by five dimensionless groups, which correspond to two sets of Reynolds and Keulegan–Carpenter numbers (one set for translational and the other for rotary motion), and the phase angle  $\Phi$  between these two motions [8].

The dimensionless quantities representative of amplitude and frequency of each motion are usually defined as follows:

$$KC_t = \frac{U_{max_t}}{f_t D} = \frac{2\pi A_t}{D}, \quad KC_\theta = \frac{U_{max_\theta}}{f_\theta D} = \pi A_\theta, \quad (23)$$

$$\beta_t = \frac{f_t D^2}{\nu}, \quad \beta_\theta = \frac{f_\theta D^2}{\nu}. \quad (24)$$

where  $KC_t(KC_\theta)$  and  $\beta_t(\beta_\theta)$  are the translational (rotational) Keulegan–Carpenter number and Stokes number, respectively;  $U_{max_t}(U_{max_\theta})$  is the maximum translational (rotational) velocity of the cylinder motion,  $D$  is the cylinder diameter, and  $\nu$  is the kinematic viscosity of the fluid [9]. We have assigned the imposed translational motion to be in the vertical direction, so that

$$y(t) = A_t \cos(2\pi f_t t), \quad (25)$$

while the rotational motion of the cylinder about its axis is described by

$$\theta(t) = A_\theta \cos(2\pi f_\theta t + \Phi), \quad (26)$$

with counterclockwise rotation corresponding to positive  $\theta$ .

**3.1. The Geometry of Flow Domain**

A computational domain extending  $30D \times 30D$  is going to be simulated.

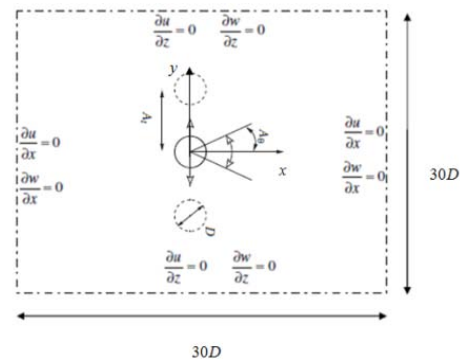


Figure 5. Schematic of the problem geometry and boundary conditions of a flow domain.

For our study, the Keulegan–Carpenter and Reynolds numbers for the translational motion were held fixed at values of  $\pi$  and  $200 \times 2^{1/2}$ , respectively. The frequency of the rotational oscillation was the same as for the translational oscillation, i.e.,  $f_t = f_\theta$ , while the amplitude of the rotational motion was set so as to make the peak tangential speed on the surface

of the cylinder the same as the peak translational speed, i.e.,  $A_\theta = 1$  rad [9]. The phase difference between translational and rotational oscillations is considered 180 radians. The resolution of the cylinder diameter is  $40l_u$  which is consistent with the one used successfully in [1]. By choosing this number of lattices for the diameter of the cylinder, the domain size according to figure 5 is  $1201 \times 1201$ .

The inlet boundary condition is a flow boundary condition, with a fixed parabolic velocity profile.

$$U(0, y) = 4U_m y(H - y)/H^2, \quad V = 0 \quad (27)$$

To simulate this boundary condition, Zou and He boundary condition on a flow boundary is used.

### 3.2. Curved Solid Boundary Condition

FH boundary condition is used for curved solid boundaries.

### 3.3. Outlet Boundary Condition

Using second-order differencing for the null first partial derivative of distribution function the following relation is obtained for the distribution function:

$$\frac{\partial f}{\partial x_{i \max}} = -\frac{3f_{i \max} - 4f_{i \max-1} + f_{i \max-2}}{2\Delta x} = 0 \Rightarrow f_{i \max} = \frac{1}{3}(4f_{i \max-1} - f_{i \max-2}). \quad (28)$$

### 3.4. Numerical Results

The vorticity contours for the instant when the cylinder is at its maximum vertical position and most negative angular displacement is shown in figure 6. The direction of rotation of the vortices will result in their being strained and directed to only one side of the cylinder and perpendicular to its translation axis.

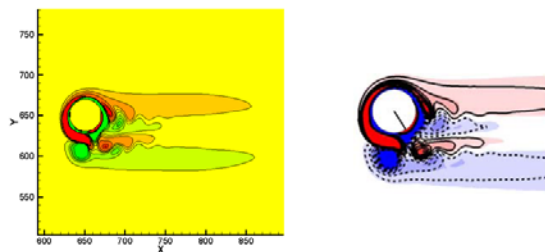


Figure 6. Vorticity contours of flow due to translational and rotational oscillation of a circular cylinder. Right: numerical results of [9], Left: numerical results of the present study.

As can be seen in figure 6 the produced vortices are spread out to right which exert a trust to the cylinder, forcing it to move to the opposite (left) direction.

Drag coefficient as a function of time is drawn in figure 7. As can be seen from figure 7 the drag coefficient of this problem is always negative which means a force is exerted in the opposite direction of the flow jet, and after three time periods ( $3T$ ) the variation of drag coefficient as a function of time becomes semi-steady. Trust force is a propulsion force, which lets the cylinder experience a locomotion movement.

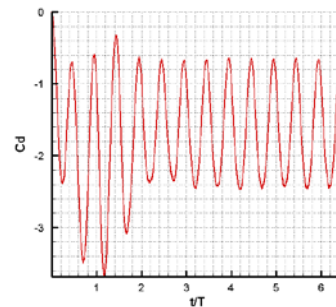


Figure 7. Drag coefficient as a function of time using FH boundary condition for moving curved solid boundaries

### 4. Simulation of Fish-like Locomotion

To model a two dimensional fish-like body a NACA-0012 foil is used. At first the airfoil is motionless and the fluid around the airfoil is stationary. The airfoil goes under a steady undulation. Due to the undulation of the airfoil a flow is produced round the airfoil. Through the interaction of the deforming body and the fluid around the body an external force makes the deforming body to cruise with a mean velocity [10]. The plunge motion of airfoil shown in Figure 8 can be expressed by

$$h = h_0 c \cos(\omega t), \quad (29)$$

where  $h$  means the instantaneous position of the airfoil,  $h_0$  is the dimensionless stroke amplitude,  $c$  denotes the chord length of the airfoil, and  $\omega$  is the flapping frequency.

Inspired by the hydrodynamics of fish-like swimming, the profile of the flexible airfoil varying over time can be expressed by:

$$y = -a_0 c x^2 \cos(\omega t + \phi), \quad (30)$$

where  $a_0$  is the dimensionless flexure amplitude and  $\phi$  denotes the phase angle [12] (figure 8).

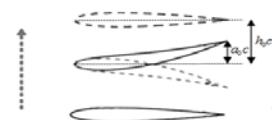


Figure 8. Plunge and deflection motion of a flexible airfoil, with  $\pi/2$  phase difference between Plunge and deflection motions

**4.1. Flow Domain Characteristics**

In reference [11] Wu, J., Shu, C. and Zhang, Y. H. have used the following flow parameters to control the motion of the airfoil to simulate a flow over a flexible airfoil:  $h_0 = 0.4$ ,  $a_0 = 0.3$ ,  $\phi = \pi/2$ ,  $\omega = 0.4$  and  $Re = 100$ .

In this study we are going to use these parameters for our flexible airfoil. The Reynolds number bases on the chord length and the maximum velocity of the oscillation of the head of airfoil. The phase difference between the plunge and deflection motions is  $\pi/2$ . The drag and lift coefficients are defined with the following relations:

$$C_D = \frac{F_x}{\frac{1}{2} \rho U_{max}^2 c} \tag{31}$$

$$C_L = \frac{F_y}{\frac{1}{2} \rho U_{max}^2 c} \tag{32}$$

We appoint the resolution of the flow domain to  $1001 \times 801$  and the chord length of the airfoil is chosen to be  $200l_u$ . The coordinate of the head of the airfoil is adjusted to the center of the flow domain.

**4.2. Numerical Results of Flow over a Flexible Airfoil with a Plunge and Deflection Motion**

In figure 9 drag coefficient is shown as a function of time. As can be seen from figure 9 the majority of drag coefficient is in negative part. Negative nature of drag coefficient means that the drag force plays as a trust force and tries to propel the flexible airfoil.

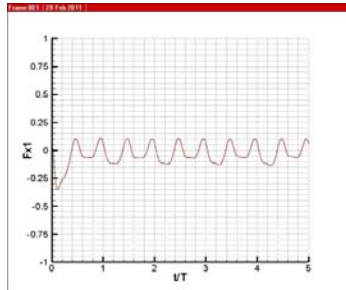


Figure 9. Drag coefficient as a function of time for a flexible airfoil with plunge motion for 5 time period.

As can be seen from figure 9 just after one time period the variation of drag coefficient becomes periodic. In figure 10 the drag coefficient as a function of time is shown for just one time period for more illustration. As can be seen from figure 10 the drag coefficient is much more in negative part than is positive part.

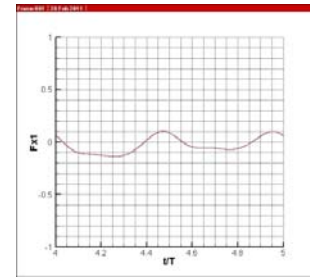


Figure 10. Drag coefficient as a function of time in one time period.

In figure 11 the instantaneous vorticity contours in three sections ( $T$ ,  $0.2T$  and  $0.4T$ ) of a time period are shown. As can be seen from figure 11 due to undulation motion of the airfoil, vortices which are produced from tail of the airfoil are stretching from tail of the airfoil to right, so that the reaction of vortex stretching causes a force to the airfoil in the opposite direction of the stretched vortices and causes the airfoil to move to left. A propulsion force was exerted without any means of external sources just because of undulation motion of the airfoil and causes the airfoil to move in the forward direction.

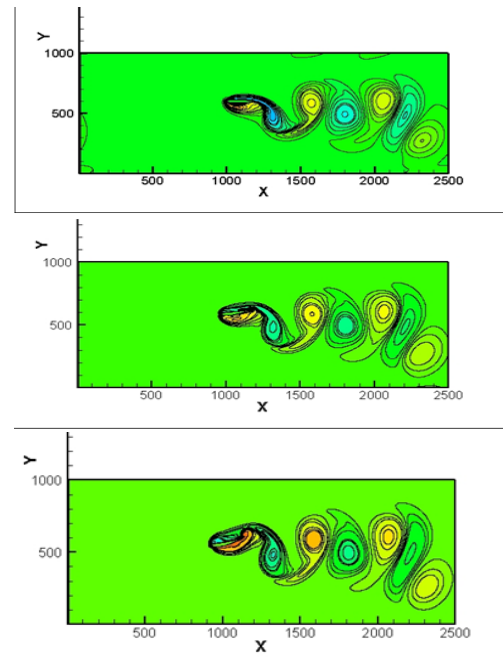


Figure 11. Vorticity contours in three sections ( $T$ ,  $0.2T$  and  $0.4T$ ) of a time period for flow over a flexible moving airfoil with a plunge and deflection motion.

By solving the dynamical equation of motion in the longitudinal direction of airfoil ( $x$  direction) implementing Euler's numerical method (equation

(33)) the path line of the centre of mass can be drawn (figure 12).

$$u_{\text{new}} = u_{\text{old}} + \Delta t.F_x/m \quad (33)$$

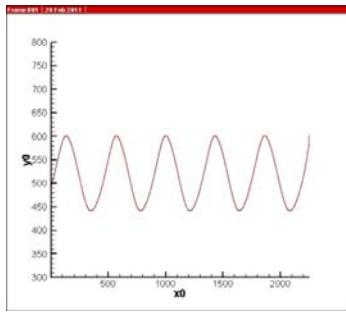


Figure 12. Path line of the centre of mass of the airfoil.

The velocity of centre of mass of the airfoil as a function of time is shown in figure 13. As can be seen from figure 13 the velocity of the centre of mass of the airfoil is always negative which means the force exerted on the airfoil via the fluid, is a propulsion force and causes the airfoil to move in the forward direction.

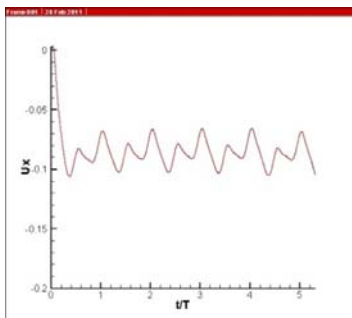


Figure 13. X-velocity component of the centre of mass of the airfoil.

#### Corresponding Author:

Dr. Mojtaba Beigzadeh-abbassi  
Department of Mechanical Engineering  
Sirjan University of Technology, Sirjan, Iran  
E-mail: [m.r.beigzadeh@gmail.com](mailto:m.r.beigzadeh@gmail.com)

#### References

1. Sukop, M.C. and Thorne, D.T. Lattice Boltzmann Modeling, An Introduction to Geoscientists and Engineers. Springer, 2006.
2. Chen, Sh. and Doolen, G. D. Lattice Boltzmann Method for Fluid Flows. Annu. Rev. Fluid Mech. 1998; 30(1): 329–64.

3. Zhou, J.G. Lattice Boltzmann Methods for Shallow Water Flows. Springer-Verlag, Berlin, Heidelberg, 2004.
4. Filippova, O. and Hanel, D. Grid Refinement for Lattice-BGK Models. J. Com. Phys. 1998; 147(1): 219–228.
5. Mei, R., Luo, L.S. and Shyy, W. An Accurate Curved Boundary Treatment in the Lattice Boltzmann Method. J. Comp. Phys. 1999; 155(2): 307–330.
6. Zou, Q. and He, X. On Pressure and Velocity Boundary Conditions for the Lattice Boltzmann BGK Model. Phys. Fluids J. 1996; 9(6):1591-1599.
7. Deladisma, M.D. Accuracy and Enhancement of the Lattice Boltzmann Method for Application to a Cell-Polymer Bioreactor System. Ph.D. Dissertation, Dept. of Mech. Eng., Georgia Institute of Tech., May, 2006.
8. Blackburn, H. M., Elston J. R. and Sheridan J. Bluff-body Propulsion Produced by Combined Rotary and Translational Oscillation. Phys. Fluids J. 1999; 11(1): 4-6.
9. Nazarinia, M., Jacono, D.L., Thompson, M.C. and Sheridan, J. The Three-dimensional Wake of a Cylinder Undergoing a Combination of Translational and Rotational Oscillation in a Quiescent Fluid. Phys. Fluids J. 2009; 21(6): 1-7.
10. Yan, Y., Wu, G.H., Yu Y.L. and Tong Bing-Gang Two-dimensional Self-Propelled Fish Motion in Medium: An Integrated Method for Deforming Body Dynamics and Unsteady Fluid Dynamics. Chin.Phys.Lett. 2008; 25(2): 597-600.
11. Wu, J., Shu, C. and Zhang, Y. H Simulation of Incompressible Viscous Flows around Moving Objects by a Variant of Immersed Boundary-lattice Boltzmann Method. Int. J. Numer. Meth. Fluids. 2010; 62(3): 27–354.
12. Wu, J., Shu, C. and Zhang, Y. H. Simulation of Incompressible Viscous Flows around Moving Objects by a Variant of Immersed Boundary-lattice Boltzmann Method. Int. J. Numer. Meth. Fluids. 2010; 62(3): 27–354.
13. Yan, Y., Wu, G.H., Yu Y.L. and Tong Bing-Gang Two-dimensional Self-Propelled Fish Motion in Medium: An Integrated Method for Deforming Body Dynamics and Unsteady Fluid Dynamics. Chin.Phys.Lett. 2008; 25(2): 597-600.

1/25/2012